Palaeogeography, Palaeoclimatology, Palaeoecology xxx (2014) xxx–xxx

Contents lists available at ScienceDirect

Palaeogeography, Palaeoclimatology, Palaeoecology

journal homepage: www.elsevier.com/locate/palaeo

A Middle–Late Triassic (Ladinian–Rhaetian) carbon and oxygen isotope record from the Tethyan Ocean

Giovanni Muttoni [a,*], Michele Mazza [a], David Mosher [b], Miriam E. Katz [b], Dennis V. Kent [c,d], Marco Balini [a]

[a] Dipartimento di Scienze della Terra "Ardito Desio", Universita' di Milano, via Mangiagalli 34, 20133 Milan, Italy
[b] Department of Earth and Environmental Sciences, Rensselaer Polytechnic Institute, Troy, NY 12180, USA
[c] Department of Earth and Planetary Sciences, Rutgers University Piscataway, NJ 08854, USA
[d] Lamont-Doherty Earth Observatory, Palisades, NY 10964, USA

ARTICLE INFO

Article history:
Received 4 October 2013
Received in revised form 15 January 2014
Accepted 18 January 2014
Available online xxxx

Keywords:
Carbon isotopes
Oxygen isotopes
Conodonts
Magnetostratigraphy
Triassic

ABSTRACT

We obtained bulk-sediment $\delta^{18}O$ and $\delta^{13}C$ data from biostratigraphically-constrained Tethyan marine sections at Aghia Marina (Greece), Guri Zi (Albania), and Brumano and Italcementi Quarry (Italy), and revised the published chemostratigraphy of the Pizzo Mondello section (Italy). We migrated these records from the depth to the time domain using available chronostratigraphic tie points, generating Ladinian–Rhaetian $\delta^{13}C$ and $\delta^{18}O$ records spanning from ~242 to ~201 Ma. The $\delta^{18}O$ record seems to be affected by diagenesis, whereas the $\delta^{13}C$ record appears to preserve a primary signal and shows values increasing by ~1‰ in the Ladinian followed by an ~0.6‰ decrease across the Ladinian–Carnian boundary, followed by relatively constant (but oscillatory) Carnian values punctuated by a negative excursion at ~233 Ma in the early Carnian, a second negative excursion at ~229.5 Ma across the early–late Carnian boundary, and a positive excursion at ~227 Ma across the Carnian–Norian boundary. The Norian record is characterized by a long-term decreasing trend and a negative excursion at ~216 Ma. Rapid increases and decreases in $\delta^{13}C$ have been observed in the Rhaetian, but these may be at least in part due to mixing of different sources of carbonate carbon with different $\delta^{13}C$ values. Our Triassic $\delta^{13}C$ record has been compared to data from the literature, and a composite $\delta^{13}C$ record spanning the last ~242 Myr of Earth's history has been generated. This composite record shows a sequence of dated $\delta^{13}C$ trends and events that can be used for stratigraphic correlation as well as for a better understanding of the global carbon cycle in the Mesozoic–Cenozoic.

1. Introduction

Our goal in this paper is to construct a continuous oxygen and carbon isotope profile anchored to Middle–Late Triassic (Ladinian–Rhaetian) biostratigraphy and magnetostratigraphy to augment the definition of the Triassic time scale. We present new biostratigraphic (conodonts), chemostratigraphic (oxygen and carbon isotopes), and paleomagnetic data from the Middle–Late Triassic (Ladinian–Norian) Aghia Marina section, which is a well exposed and continuous marine section comprised of Tethyan pelagic limestones located on the island of Hydra in Greece (Angiolini et al., 1992). Because the Aghia Marina section is remagnetized, its bio-chemostratigraphic results cannot be directly tied to magnetic polarity reversals; nonetheless, the section remains a useful ancillary section for the definition of the Late Triassic time scale. We also present new chemostratigraphic data and a revised conodont biostratigraphy from the Late Triassic (Carnian–Norian) Guri Zi section from Albania (Muttoni et al., 2005), as well as new chemostratigraphic data from the Late Triassic (Rhaetian) Brumano and Italecmenti Quarry sections from northern Italy (Muttoni et al., 2010). Moreover, we summarize the published chemostratigraphy, magnetostratigraphy, and conodont biostratigraphy of the Carnian–Norian Pizzo Mondello section (Muttoni et al., 2004; Mazza et al., 2012a). We place these chemostratigraphic records in the numerical time domain by applying age models of sedimentation obtained by means of magnetostratigraphic correlations with the Newark Astrochronological Polarity Time Scale (APTS) (Kent and Olsen, 1999; Olsen and Kent, 1999) anchored to a Triassic–Jurassic (Rhaetian–Hettangian) boundary at ~201.5 Ma after recent numerical age estimates for the base of Central Atlantic Magmatic Province (=~age of end-Triassic Extinction; Blackburn et al., 2013). The resulting stable isotope profiles spanning ~40 Myr of the Triassic represent a significant step forward for the development of an important chemostratigraphic correlation tool in sections with insufficient magnetobiostratigraphy to determine higher-resolution age models. Finally, we integrated our Triassic $\delta^{13}C$ record with data from the literature in order to generate – and discuss – a composite record of the global carbon cycle spanning the last ~242 Myr of Earth's history.

2. The Ladinian–Norian Aghia Marina section

2.1. Geological setting and lithostratigraphy

The Aghia Marina section is located on the island of Hydra in Greece (Fig. 1). Hydra is characterized by a Permian to Jurassic sedimentary

* Corresponding author. Tel.: +39 02 503 15518.
E-mail address: giovanni.muttoni1@unimi.it (G. Muttoni).

0031-0182/$ – see front matter © 2014 Elsevier B.V. All rights reserved.
http://dx.doi.org/10.1016/j.palaeo.2014.01.018

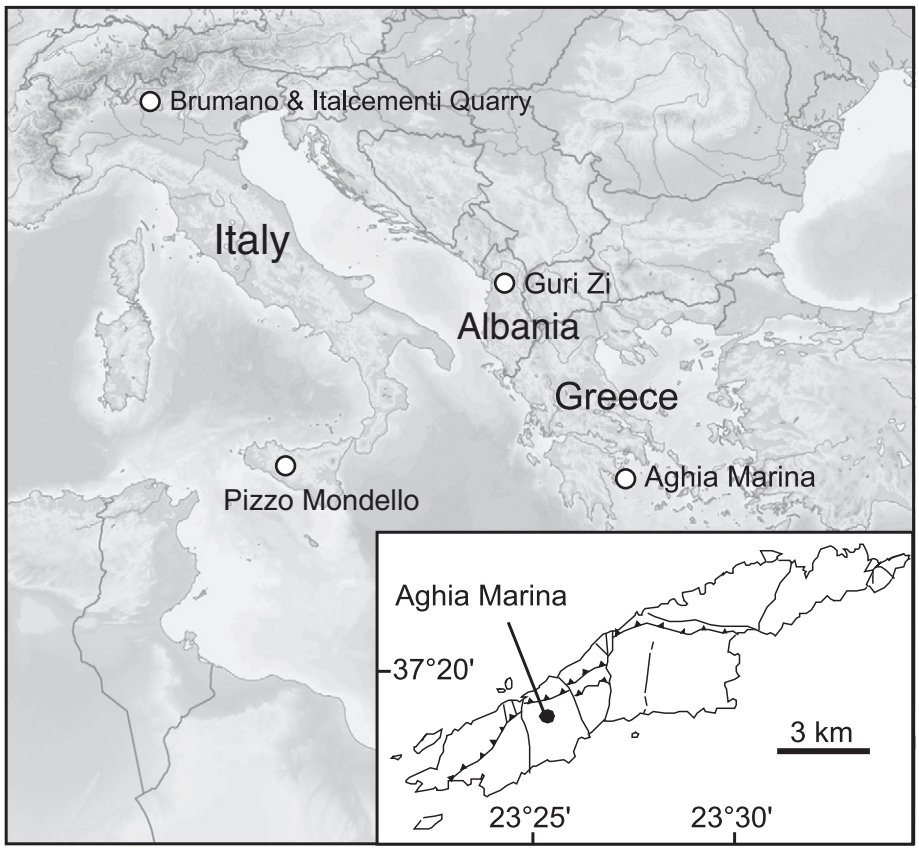

Fig. 1. Location map of the stratigraphic sections discussed in the text: Aghia Marina (Greece), Pizzo Mondello (Italy), Guri Zi (Albania), and Brumano and Italcementi Quarry (Italy). The inset shows the tectonic map of Hydra, Greece (Angiolini et al., 1992) with location of the Aghia Marina section.

succession (Renz, 1931; Angiolini et al., 1992; Balini, 1994; Muttoni et al., 1994, 1997) arranged in four major thrust sheets dissected by north–south trending faults as the result of deformation during the Late Jurassic and Cenozoic (Baumgartner, 1985; Angiolini et al., 1992). The Middle–Late Triassic (Ladinian–Norian) Aghia Marina section, first described by Angiolini et al. (1992, Section A), is located near the Aghia Marina chapel (37°19′14.07″N; 23°25′15.60″E) in the southern thrust sheet (Fig. 1; see also Angiolini et al., 1992). The section starts with an ~5 m-thick interval of thinly bedded cherts and continues with ~157 m of cm to dm-thick planar beds of gray limestones with chert nodules with occasional thin levels of red clays and meter-scale levels of calcarenites, altogether pertaining to the Adhami Limestone, overlain by ~12 m of pink and gray nodular limestones of the Rosso Ammonitico (Fig. 2).

2.2. Conodont biostratigraphy

We present a complete conodont biostratigraphic record of the Aghia Marina section (Figs. 2, 3; Supplementary Table 1) that takes into account previous results (Angiolini et al., 1992) and recent taxonomic revisions of Late Triassic conodonts (Kozur, 2003; Moix et al., 2007; Noyan and Kozur, 2007; Mazza et al., 2011, 2012a,b).

The section starts close to the Anisian–Ladinian boundary (Angiolini et al., 1992; Balini, 1994) and extends into the Ladinian, Carnian, and Norian (this study). In particular, in the interval between sample AM14 and sample AM37, the section is Ladinian (Longobardian) based on the occurrences of *Gladigondolella* sp., *Gladigondolella malayensis malayensis* Nogami, *Paragondolella inclinata* (Kovács), *Paragondolella foliata* Budurov and *Neocavitella tatrica* (Zawidzka). The Ladinian–Carnian boundary is placed at ~60 m in sample MA5 at the first occurrence of *Paragondolella polygnathiformis* (Budurov & Stefanov) (Fig. 3B), which is a proxy marker for the base of the Carnian (Mietto et al., 2012).

Above follows an early Carnian (Julian) association of *Paragondolella polygnathiformis*, *Paragondolella foliata*, *Paragondolella praelindae* Kozur (Fig. 3E), *Paragondolella tadpole* (Hayashi) (Fig. 3A, D), and *Carnepigondolella nodosa* (sensu Hayashi, 1968) (Fig. 3C). The interval from ~112 m in sample MA9 to ~135 m in sample AM55 is regarded as late Carnian (Tuvalian) based on the last occurrence in sample MA9 of *P. foliata* and the first occurrence in sample AM55 of *Carnepigondolella gulloae* Mazza and Rigo (Fig. 3F) [ex "*Metapolygnathus communisti* B" Krystyn, see Mazza et al. (2012a)], which is early Norian (Balini et al., 2010; Mazza et al., 2012a). The only species recovered in this Tuvalian interval are *P. polygnathiformis* and *C. nodosa*, which extend up to the early–middle Tuvalian (Martini et al., 1991; Moix et al., 2007; Balini et al., 2010; Mazza et al., 2012a).

The upper part of the section, from ~135 m in sample AM55 to ~172 m in sample AM65, dates to the early–middle Norian (Lacian–Alaunian) based on the first occurrence of *Carnepigondolella gulloae* in sample AM55 (super-adult growth stages; Fig. 3F), in association with juvenile stage specimens of *Epigondolella quadrata* Orchard (Fig. 3I, J). The interval comprised between sample AM61, located just below the base of the Rosso Ammonitico, and sample AM65 at the section top, yielded a middle Norian (Alaunian) association composed of *Norigondolella navicula* (Huckriede) (Fig. 3G), *Norigondolella steinbergensis* (Mosher) (Fig. 3H, L), *Norigondolella* sp. (Fig. 3M, N), and *Norigondolella kozuri* (Gedik) (Fig. 3K); the FO of *N. steinbergensis* in sample AM61 is here used as marker for the middle Norian. This conodont association indicates that the Ammonitico Rosso is Late Triassic in age and not Early Jurassic, as previously proposed (Angiolini et al., 1992).

The conodont color alteration index (CAI) ranges from 4 to 6.5 (Supplementary Table 1), suggesting that the succession has been subject to temperatures in excess of 300 °C (e.g., Epstein et al., 1977), which may

Please cite this article as: Muttoni, G., et al., A Middle–Late Triassic (Ladinian–Rhaetian) carbon and oxygen isotope record from the Tethyan Ocean, Palaeogeogr. Palaeoclimatol. Palaeoecol. (2014), http://dx.doi.org/10.1016/j.palaeo.2014.01.018

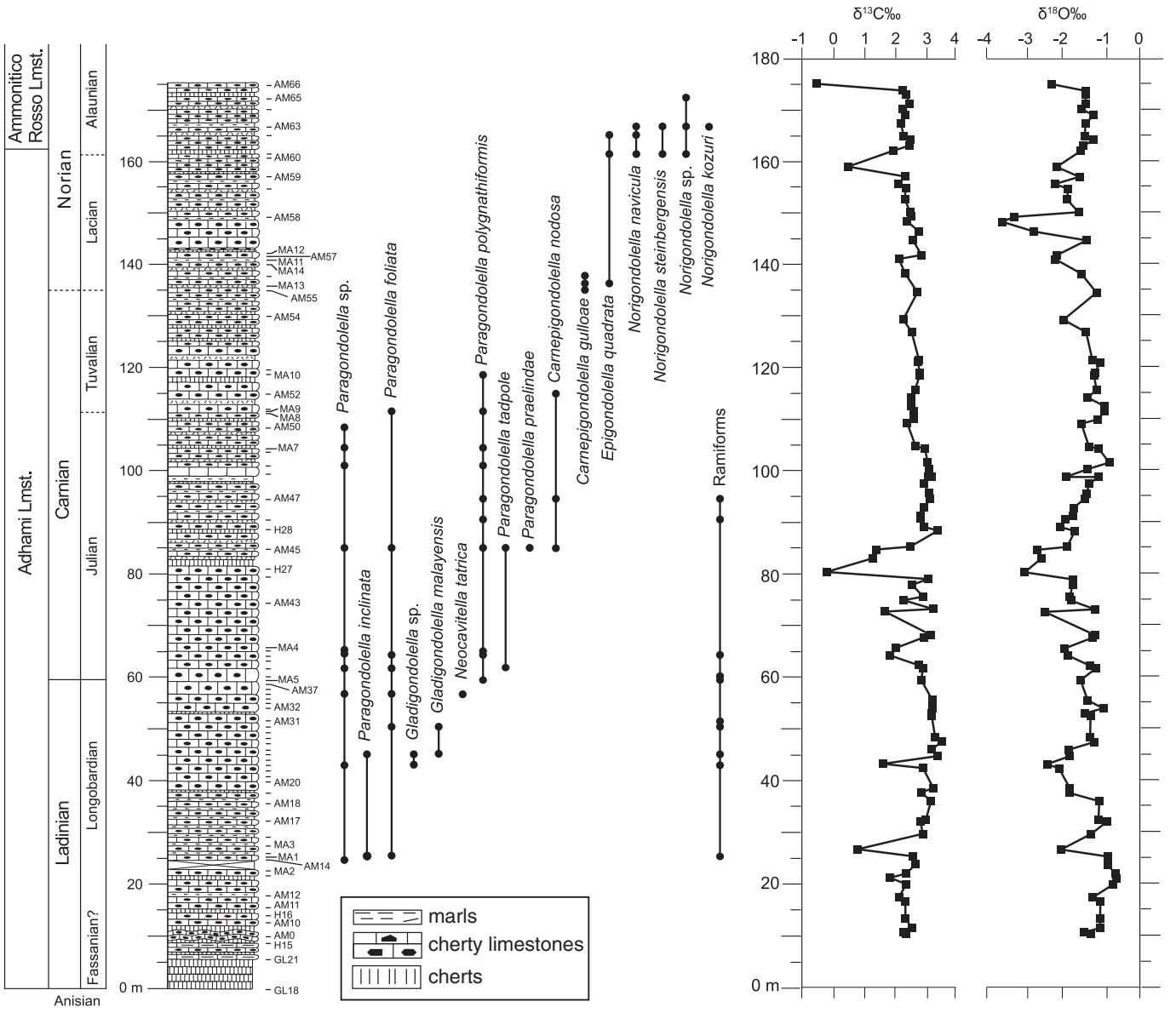

Fig. 2. Aghia Marina section. From left to the right: age, lithology, conodont biostratigraphy, and bulk-rock $\delta^{13}C$ and $\delta^{18}O$ data. See text for discussion.

have caused remagnetizations and diagenesis of the stable isotopes, as discussed below.

2.3. Paleomagnetism

Paleomagnetic samples were drilled and oriented in the field at an average sampling interval of ~0.45 m giving a total of 363 standard ~11 cm^3 specimens for analyses. The intensity of the natural remanent magnetization (NRM) is characterized by low values from the section base up to ~35 m followed by generally higher values up to ~160 m and, finally, by low values up to the section top at ~175 m (Fig. 4A). Initial susceptibility (not shown) and isothermal remanent magnetizations (IRMs) imparted in 0.3 and 2.5 T fields follow this trend with highest values in the middle part of the section (Fig. 4A). IRM acquisition curves (Fig. 4B) coupled with unblocking temperature analysis (see below) suggest the presence of a dominant low coercivity magnetite phase in association with subsidiary high coercivity hematite. Thermal demagnetization of the NRM revealed the presence of scattered initial component directions broadly oriented to the north and down (positive inclinations) in in situ coordinates and interpreted as a recent viscous overprint. Magnetic components linearly trending to the origin of the demagnetization axes were observed between ~350 °C and 550 °C or rarely 680 °C (Fig. 4C). These high temperature magnetic components are bipolar and oriented northerly and down (positive inclinations) or southerly and up (negative inclinations) in in situ coordinates between the section base and meter level ~35, and from meter level ~160 to the section top (Fig. 4D, upper and lower panels, respectively), whereas they tend to be scattered mainly in the southeast quadrant in the intervening part (~35–160 m) of the section (Fig. 4D, middle panel). After correction for homoclinal bedding tilt, these components become oriented northerly and up or southerly and down in the lower and upper sub-sections, and streaked between easterly and southerly down in the intervening middle sub-section (Fig. 4D).

The bipolar northerly and up or southerly and down component directions in the lower and upper sub-sections are similar to component directions previously observed in Middle Triassic sections on Hydra and considered primary in origin, acquired in the northern hemisphere during reverse or normal geomagnetic field polarities, respectively (Muttoni et al., 1994, 1997). Consequently, virtual geomagnetic pole (VGP) latitudes have been calculated for these components to unravel a sequence of (poorly defined) magnetic polarity reversals (Fig. 4A). We interpret the single polarity-dominated median portion of the

Please cite this article as: Muttoni, G., et al., A Middle–Late Triassic (Ladinian–Rhaetian) carbon and oxygen isotope record from the Tethyan Ocean, Palaeogeogr. Palaeoclimatol. Palaeoecol. (2014), http://dx.doi.org/10.1016/j.palaeo.2014.01.018

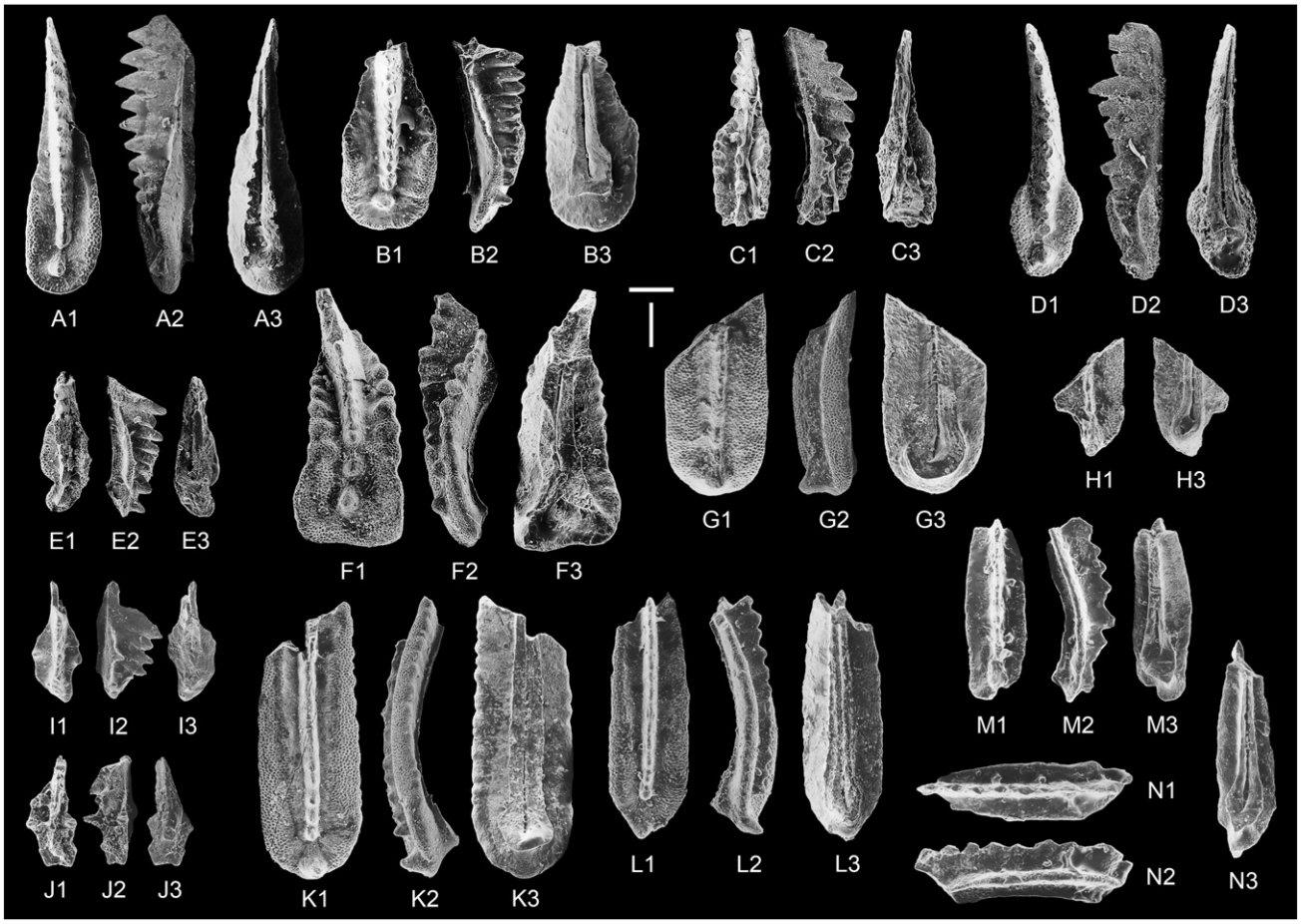

Fig. 3. SEM micro-photographs of conodont species from the Aghia Marina section. Scale bars are 100 μm; all specimens are at the same scale. (A) *Paragondolella tadpole*, mature growth stage, sample AM39; (B) *Paragondolella polygnathiformis*, mature growth stage, sample AM41; (C) *Carnepigondolella nodosa*, mature growth stage, sample NA45; (D) *Paragondolella tadpole*, mature growth stage, sample AM45; (E) *Paragondolella praelindae*, juvenile growth stage, sample AM45; (F) *Carnepigondolella gualloae*, super-adult growth stage, sample AM55; (G) *Norigondolella navicula*, mature growth stage, sample AM61; (H) *Norigondolella steinbergensis*, sub-mature growth stage, sample AM61; (I) *Epigondolella quadrata*, juvenile growth stage, sample AM61; (J) *Epigondolella quadrata*, juvenile growth stage, sample AM62; (K) *Norigondolella kozuri*, mature growth stage, sample AM63; (L) *Norigondolella steinbergensis*, mature growth stage, sample AM63; (M) *Norigondolella* sp., sub mature growth stage, sample AM65; (N) *Norigondolella* sp., sub mature growth stage, sample AM65. 1: upper view; 2: lateral view; 3: lower view.

section (from 35 to 160 m) as affected by a pervasive remagnetization event associated with high NRM, IRM, and susceptibility values. The high conodont CAI values further support the hypothesis that the succession suffered from high thermal alteration.

2.4. Geochemistry

Rock samples for bulk carbonate stable isotope analyses ($\delta^{18}O$, $\delta^{13}C$) were cut with a Buehler Isomet Low Speed Saw to avoid veins. Samples were broken into millimeter fragments using a rock hammer, and then crushed for 15 to 20 min, or until completely powdered, at low speed in a Fritsch Ball Mill or an Across International HQ-NO4 Vertical Planetary Ball Mill. Between each crushing, the agate bowl (lid, rubber washer, and cup) was cleaned and rinsed thoroughly to remove any remaining powdered sample. Stable isotopes were measured on bulk sediment samples in the Stable Isotope Lab at Rutgers University using a multiprep peripheral device and analyzed on an Optima mass spectrometer. Samples were reacted in 100% phosphoric acid at 90 °C for 13 min. Values are reported relative to V-PDB through the analysis of an internal standard calibrated with NBS-19 (1.95‰ for $\delta^{13}C$), as reported by Coplen (1995).

Diagenesis can be an issue particularly in the older geologic record, including in the Triassic. Unrealistically low values of $\delta^{13}C$ and $\delta^{18}O$ may indicate diagenesis. However, covariation of $\delta^{13}C$ and $\delta^{18}O$ can occur both in unaltered and diagenetically altered sediments and rocks, and therefore does not provide a reliable indicator of diagenesis and should only be used as a last resort; in addition, $\delta^{18}O$ may be diagenetically altered, while $\delta^{13}C$ in the same sample retains its primary signal (Marshall, 1992). Classic examples of primary covariation in $\delta^{13}C$ and $\delta^{18}O$ include the Paleocene–Eocene Thermal Maximum and the Eocene hyperthermals. We rely on correlations among sites to indicate that isotopic trends and events are primary signals.

The Aghia Marina $\delta^{13}C$ record fluctuates around a long-term mean of ~2.5‰ (standard deviation of 0.6‰). This includes an initial Ladinian increase of ~1‰, from 2.4‰ to 3.4‰ (~0–50 m), followed by a gradual return to ~2.4‰ at ~110 m, with relatively constant values persisting to the top of the section (Fig. 2). Superimposed on these long-term trends are several excursions towards lower values, most of which are defined by only one sample (at 27 m, 43 m, 158 m, 175 m) save for the notable excursion at ~80 m where the $\delta^{13}C$ decreases by ~3‰ to a minimum of −0.24‰ (Fig. 2). The $\delta^{18}O$ record fluctuates around a mean of ~−1.6‰ (standard deviation of 0.5‰) with short excursions towards lower values (at 27 m, 43 m, 80 m, 158 m, 175 m) where the $\delta^{13}C$ excursions were also found, plus one at 149 m where a minimum of −3.6‰ is reached (Fig. 2).

The Adhami Limestone from Aghia Marina suffered temperatures in excess of 300 °C during diagenesis, as suggested by the conodont CAI ranging from 4 to 6.5 and the presence of a pervasive remagnetization overprint isolated in the median portion of the section (see above).

Please cite this article as: Muttoni, G., et al., A Middle–Late Triassic (Ladinian–Rhaetian) carbon and oxygen isotope record from the Tethyan Ocean, Palaeogeogr. Palaeoclimatol. Palaeoecol. (2014), http://dx.doi.org/10.1016/j.palaeo.2014.01.018

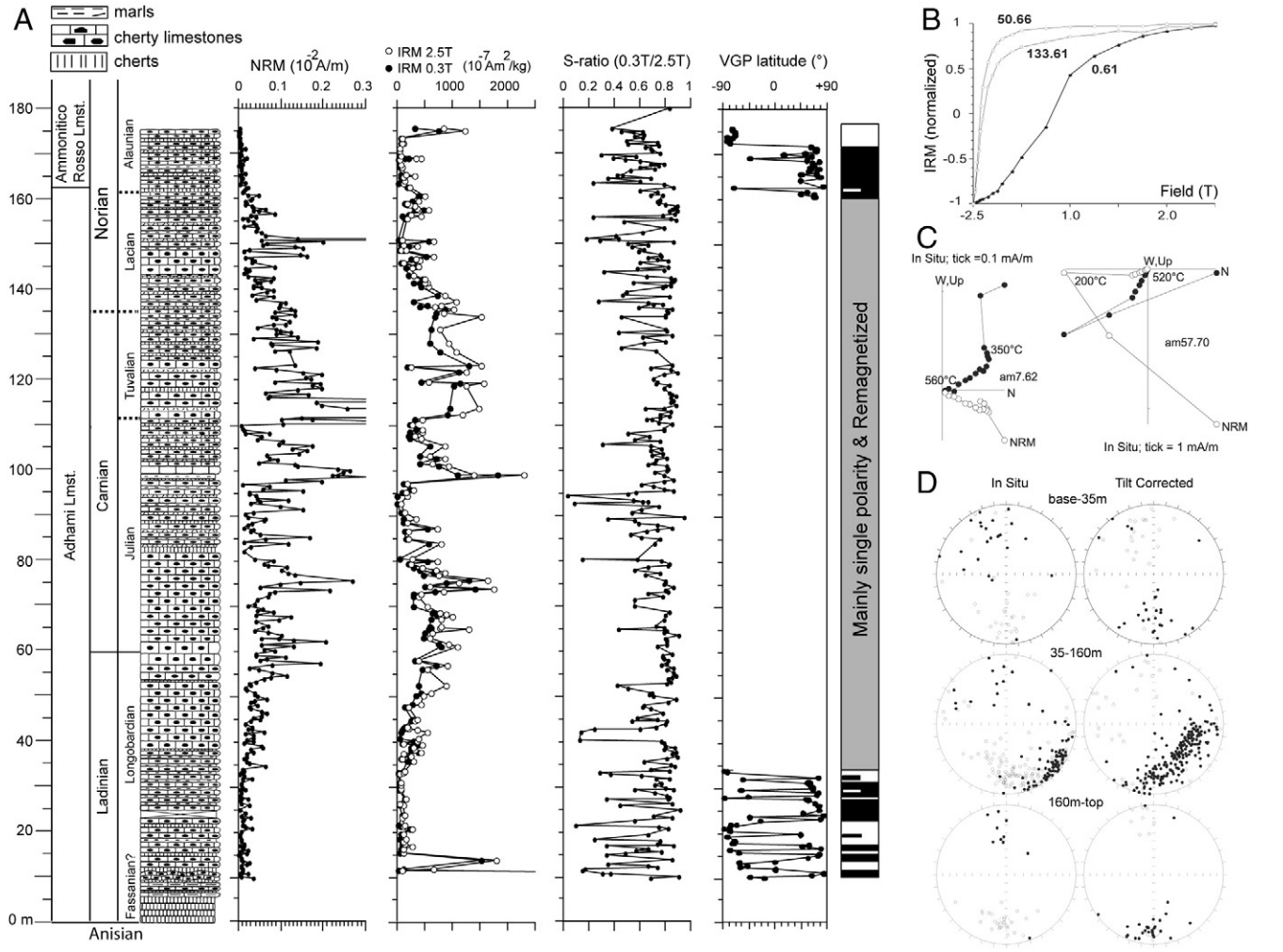

Fig. 4. Paleomagnetic data of the Aghia Marina section: (A) from left to the right: age and lithology, natural remanent magnetization (NRM), isothermal remanent magnetizations (IRM) at 0.3 T and 2.5 T (C), S-ratio (0.3 T/2.5 T), virtual geomagnetic pole (VGP) latitudes and magnetic polarity stratigraphy (black is normal, white is reverse, gray is unknown). (B) Isothermal remanent magnetization acquisition curves. (C) Vector end-point demagnetization diagrams (closed symbols are projections onto the horizontal plane and open symbols onto the vertical plane in geographic [in situ] coordinates). (D) Equal-area projections of magnetic component directions before (in situ) and after bedding tilt correction (closed symbols are projections onto the lower hemisphere and open symbols onto the upper hemisphere).

Hence, it is possible that the isotope records from Aghia Marina are affected by diagenesis, especially the oxygen signal, generally considered less resistant to diagenetic alteration than carbon. To test this hypothesis, we compare the $\delta^{13}C$ and $\delta^{18}O$ data from Aghia Marina with isotope data from the Pizzo Mondello section in Sicily (Muttoni et al., 2004), which is characterized by a relatively simple diagenetic history as testified by the presence of conodonts with CAI = 1 (Mazza et al., 2010) and of primary magnetic component directions (Muttoni et al., 2004).

3. The Carnian–Norian Pizzo Mondello section

The first magnetostratigraphic and biostratigraphic study of an expanded Carnian–Norian boundary section at Pizzo Mondello in Sicily (37°37′48.79″N; 13°24′21.98″E; Fig. 1) was published by Muttoni et al. (2001). Muttoni et al. (2004) refined these initial findings, and extended the analysis upwards into the Norian, attaining a total ~430 m-thick record of 27 polarity magnetozones from PM1r to PM12r (Fig. 5), and a biostratigraphic record across the Late Carnian–Norian; these authors also obtained oxygen and carbonate carbon isotope data through the section (Fig. 5). The conodont taxonomy and biostratigraphy of the section have been revised since then (Nicora et al., 2007; Balini et al., 2012; Mazza et al., 2012a,b), albeit the position of the Carnian–Norian boundary remained close to where it was placed by Muttoni et al. (2001) within magnetozone PM4r (Fig. 5). In this paper, we adopt the updated biostratigraphic scheme of Mazza et al. (2012a) as summarized in Fig. 5.

Muttoni et al. (2004) correlated the sequence of 27 polarity magnetozones to the Newark Astrochronological Polarity Time Scale (APTS). According to their preferred correlation option #2 (Supplementary Fig. 1A), the Carnian–Norian boundary based on conodonts, which falls within magnetozone PM4r together with its closely associated $\delta^{13}C$ increase (see below), should correspond to Newark magnetozone E7 at ~227 Ma (adopting Newark astrochronology with an updated age for the Triassic–Jurassic boundary at ~201.5 Ma; Blackburn et al., 2013), similar to what was previously concluded by Channell et al. (2003) based on the correlation between the Silicka Brezova section from Slovakia and the Newark APTS. This conclusion was substantially confirmed by subsequent data from Guri Zi (Muttoni et al., 2005; see below).

Stable carbon ($\delta^{13}C$) and oxygen ($\delta^{18}O$) isotopes were analyzed in 115 samples of bulk carbonate (Fig. 5; data from Muttoni et al., 2004). The analyzed limestones, with simple diagenetic history testified by conodont CAI = 1 (Mazza et al., 2010) and of primary magnetic component directions, should provide a carbon isotope record reflecting a global signal with possible influence of regional variability in the western Tethys during the Carnian–Norian, because up to 40% of the Scillato

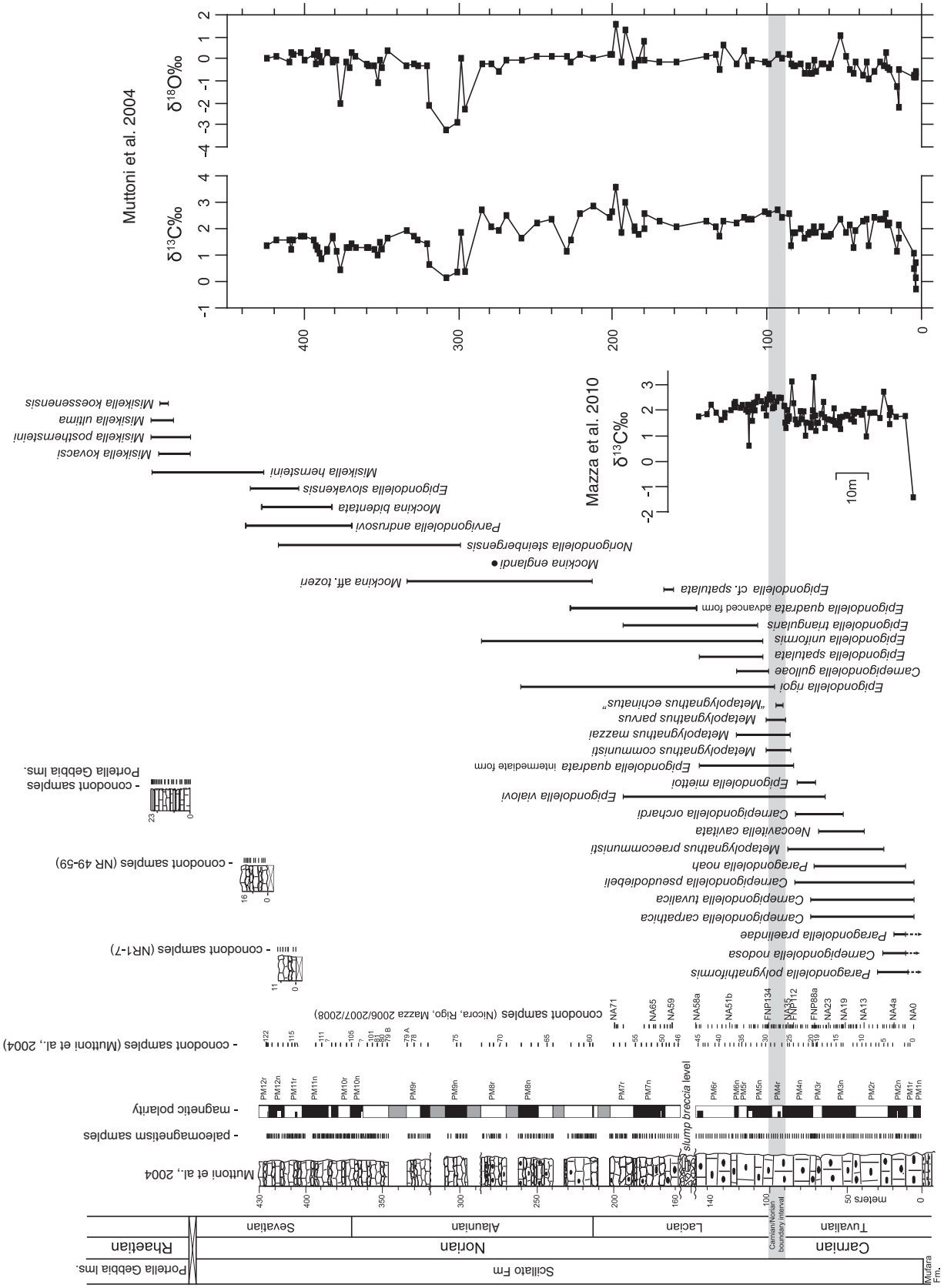

Fig. 5. Pizzo Mondello section. From left to the right: age, lithology, magnetostratigraphy, conodont biostratigraphy, and bulk-rock $\delta^{13}C$ and $\delta^{18}O$ data. See also Mazza et al. (2012a) for a detailed biostratigraphic record.

Formation (Cherty Limestone *Auctorum*) sediment volume at Pizzo Mondello consists of calcareous nannofossils and the remainder volume of micrite re-deposited from adjacent shallow-water carbonate platforms (Preto et al., 2012). Among the several features observed in the carbon isotope curve are: 1) a (partial) excursion to low values (<0‰) at the section base that is followed by values of ~2.5–2.0‰ up to 90 m; 2) an increase of ~0.8‰ located very close to the Carnian–Norian boundary interval at 90–100 m, from an average value of ~2‰ below the boundary to ~2.8‰ above the boundary; and 3) in a longer context, a trend from lower average values of ~1.7‰ in the late Carnian (Tuvalian) to typical values of ~2.3‰ observed from the Carnian–Norian boundary at 90–100 m up to ~280 m in the middle Norian (Alaunian) (Fig. 5). At ~290–320 m in the middle Norian there is a negative excursion of ~2‰ in $\delta^{13}C$ (and of ~3‰ in $\delta^{18}O$). Above this excursion, higher $\delta^{13}C$ values averaging 1.4‰ are maintained up to the section top in the late Norian (Sevatian); this average is ~0.6‰ lower than just below the excursion (Fig. 5). More recent $\delta^{13}C$ isotope analyses have been performed on 108 bulk carbonate samples from the lower 143 m of the section across the Carnian–Norian boundary (Mazza et al., 2010). The results are in general agreement with those of Muttoni et al. (2004), including the low values at the base, positive $\delta^{13}C$ shift across the Carnian–Norian boundary, and subsequent decrease in $\delta^{13}C$ (Fig. 5).

The $\delta^{18}O$ record displays a single prominent negative excursion at 290–320 m in the middle Norian (Alaunian) correlative with a $\delta^{13}C$ negative excursion of similar magnitude (Fig. 5). In general, the $\delta^{18}O$ values from Pizzo Mondello are much higher than broadly coeval values from Aghia Marina (Fig. 2), which suggest that diagenesis may have altered the $\delta^{18}O$ signal, especially at Aghia Marina, which suffered diagenetic temperatures in excess of 300 °C (see also Discussion above).

4. The Carnian–Norian Guri Zi section

The Guri Zi section is located 14 km southeast of the town of Shkodra in northern Albania (42°03′00″N; 19°34′48″E) (Fig. 1). The magnetostratigraphy and conodont biostratigraphy of the section have been described by Muttoni et al. (2005) who found a total of 14

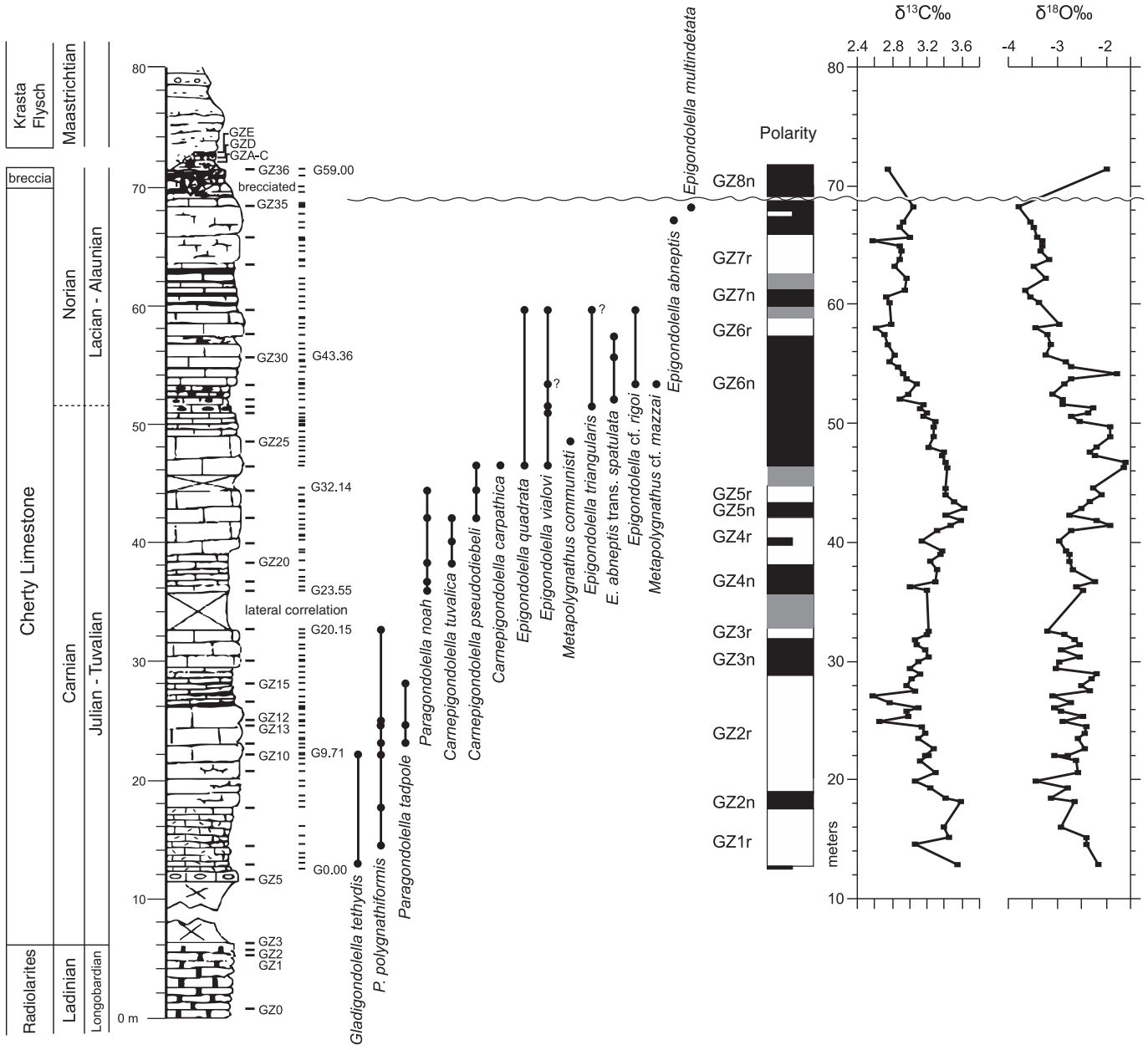

Fig. 6. Guri Zi section. From left to the right: age, lithology, conodont biostratigraphy, magnetostratigraphy, and bulk-rock $\delta^{13}C$ and $\delta^{18}O$ data. See text for discussion.

Please cite this article as: Muttoni, G., et al., A Middle–Late Triassic (Ladinian–Rhaetian) carbon and oxygen isotope record from the Tethyan Ocean, Palaeogeogr. Palaeoclimatol. Palaeoecol. (2014), http://dx.doi.org/10.1016/j.palaeo.2014.01.018

magnetozones, from GZ1r to GZ8n (Fig. 6), associated with conodonts straddling the Carnian–Norian boundary interval. The biostratigraphy of the section is here revised (Fig. 6) after recent taxonomic updates of Late Triassic conodonts (Nicora et al., 2007; Mazza et al., 2012a,b) using the iconographic material provided in Muttoni et al. (2005). Some specimens originally classified as *Paragondolella noah* and *Paragondolella noah* trans. *Paragondolella carpathica* are split into *Carnepigondolella tuvalica* Mazza and Rigo (samples GZ20, GZ21, and GZ22) and *Carnepigondolella pseudodiebeli* (samples GZ22, GZ23 and GZ24). The specimens of *Paragondolella carpathica* and *Epigondolella primitia* in sample GZ25 are here considered to belong to *Metapolygnathus communisti* Hayashi. *Metapolygnathus nodosus* Hayashi is split into *Carnepigondolella carpathica*, *Epigondolella quadrata* and *Epigondolella vialovi* Buryi (all in sample GZ24). The figured specimens of *Epigondolella abneptis* (Huckriede) and of *E. abneptis–Epigondolella spatulata* Hayashi are split into *E. vialovi* (samples GZ26, GZ27, GZ29, and GZ32), *Epigondolella triangularis* (Orchard) (samples GZ27 and GZ32), *Metapolygnathus* cf. *mazzai* Karádi, Kozur and Görög (sample GZ29), and *Epigondolella* cf. *rigoi* Noyan & Kozur (samples GZ29 and GZ32). The specimens of *E. abneptis* in sample GZ34 and of *E. abneptis–E. spatualata* in samples GZ28, GZ30, and GZ31 are not figured in Muttoni et al. (2005), and thus they are retained with the original taxonomic attribution. Based on this new biostratigraphic scheme, the Carnian–Norian boundary falls within magnetozone GZ6n (as in Muttoni et al., 2005) between the first occurrence of *E. quadrata* and the first occurrence of *E. triangularis* (Fig. 6).

The updated conodont biostratigraphy of Guri Zi correlates well with biostratigraphic records of Pizzo Mondello and Aghia Marina; all these sections are characterized by the presence of recently established species useful to approximate or possibly define the Carnian–Norian boundary (i.e., *Epigondolella* cf. *rigoi* and *Carnepigondolella gulloae*). We adopt the magnetostratigraphic correlation scheme of Hounslow and Muttoni (2010) between Guri Zi and Pizzo Mondello, which supersedes the original correlation of Muttoni et al. (2005), while Pizzo Mondello is correlated to the Newark APTS using correlation option #2 of Muttoni et al. (2004) [also used in Hounslow and Muttoni, 2010]. These correlations (Supplementary Fig. 1B) indicate that the conodont Carnian–Norian boundary at Guri Zi and Pizzo Mondello falls within Newark magnetozone E7 at ~227 Ma.

The $\delta^{13}C$ and $\delta^{18}O$ data from Guri Zi have been obtained using methods and standards outlined for the Aghia Marina section (see above). The $\delta^{13}C$ record of Guri Zi fluctuates between ~3.6‰ and ~2.6‰ (Fig. 6). The stratigraphic interval across the Carnian–Norian boundary displays an increasing trend followed by a decreasing trend in the Norian (Fig. 6), which is reminiscent of the Carnian–Norian boundary record at Pizzo Mondello (see above). $\delta^{18}O$ values (Fig. 6) are much lower than coeval values from Aghia Marina (Fig. 2) and Pizzo Mondello (Fig. 5), suggesting that diagenesis may have variably altered the $\delta^{18}O$ signal, especially at Guri Zi and Aghia Marina.

5. The Rhaetian Brumano and Italcementi Quarry sections

The magnetostratigraphy and conodont biostratigraphy of the ~427 m-thick Brumano section (45°50′49″N; 9°29′50″E) and the ~160 m-thick Italcementi Quarry section (45°46′43″N; 9°31′11″E) from the Southern Alps of Italy (Fig. 1) have been studied by Muttoni et al. (2010). These sections crop out in close contiguity and cover an ~520 m-thick composite stratigraphic interval from the Late Triassic (Rhaetian) Zu1 member of the Zu Limestone across the overlying Zu2 to Zu3c members of the Zu Limestone of still Rhaetian age and up to the Malanotte and Albenza formations of Early Jurassic (Hettangian) age (Fig. 7; see Muttoni et al., 2010 for details). The Rhaetian age attribution was based on the occurrence of conodont *Misikella posthernsteini* (Kozur & Mock) in the Zu1 member at Brumano (Fig. 7; see also Muttoni et al., 2010), whereas the Triassic–Jurassic (T–J) boundary was placed at the base of the Malanotte Formation in the Italcementi Quarry section (and the nearby Malanotte section) between the disappearance of Rhaetian pollen such as *Rhaetipollis germanicus* and the acme of *Kraeuselisporites reissingeri* associated with other diagnostic Hettangian pollen typical of the Malanotte Formation (Fig. 7; Muttoni et al., 2010).

Magnetic component directions of presumed depositional age record a sequence of 9 normal and reverse polarity magnetozones from Brumano and Italcementi Quarry labeled from BIT1n to BIT5n that have been correlated to the Newark APTS (Muttoni et al., 2010) here anchored to a Triassic–Jurassic boundary at ~201.5 Ma after recent age estimates from Blackburn et al. (2013) (Fig. 7). The Norian–Rhaetian boundary (as defined by the first appearance of conodont *Misikella posthernsteini*) is tentatively placed on the Newark APTS at ~207–210 Ma (nominal age of ~209 Ma) after Muttoni et al. (2010) and Hüsing et al. (2011), implying a total duration of the Rhaetian of ~5.5–8.5 Myr, a solution that contrasts with a much shorter duration of the Rhaetian in alternative Late Triassic magneto-biostratigraphic schemes from the literature (Krystyn et al., 2002; Gallet et al., 2007).

Previous carbon isotope data (Galli et al., 2005, 2007; see also Muttoni et al., 2010) across the T–J boundary interval from the Italcementi Quarry section and the nearby and the more continuous Malanotte section showed that the T–J boundary level is characterized by a negative carbon isotope excursion with minimum values of ~-1‰ followed across much of the overlying part of the Malanotte Formation by an extended positive excursion with maximum values of ~4‰ and by a second negative excursion with a minimum value of around 2‰, whereas at the Italcementi Quarry section, the boundary level and the associated initial negative carbon isotope excursion seem to be absent (Fig. 7). Here we extend the carbon isotope study of Galli et al. (2005, 2007) into the Rhaetian and provide new oxygen isotope data.

New stable carbon ($\delta^{13}C$) and oxygen ($\delta^{18}O$) isotopes were analyzed on 107 and 51 bulk rock samples from Brumano and Italcementi Quarry, respectively, across the entire ~520 m of composite section. In general, isotope data oscillate with high amplitude: ~9‰ in $\delta^{18}O$ and ~4‰ in $\delta^{13}C$ at Brumano, and ~5‰ in $\delta^{18}O$ and ~3‰ in $\delta^{13}C$ at Italcementi Quarry (Fig. 7). The origin of this variability in $\delta^{13}C$ (and $\delta^{18}O$) data (particularly in the Brumano section) is unclear, but we note that unlike Aghia Marina, Pizzo Mondello, and Guri Zi, the Brumano and Italcementi Quarry sections are characterized by greater lithological variability (shallow-water carbonate cycles in Zu2 and Zu3c; marl and marly limestone cycles in Zu3a and Zu3b). This may have resulted in variable mixing of carbon with different isotopic compositions from different sources, such as sediments from platform tops mixing with oceanic-derived sediments to form periplatform carbonates, which can cause variable mixing of end-member isotopic values (e.g., Swart, 2008).

6. Age models of sedimentation

According to preferred correlation option #2 of Muttoni et al. (2004), the Pizzo Mondello magnetostratigraphy straddles the Newark APTS from about the base of magnetozone E5r at ~230 Ma to about the top of magnetozone E17n at ~209.5 Ma, implying a total duration of ~20.5 million years for the interval comprised between the late Carnian (Tuvalian) to close to the Norian–Rhaetian boundary (Supplementary Fig. 1A). This correlation implies a Carnian–Norian boundary in Newark magnetozone E7 at ~227 Ma (Supplementary Fig. 1A), similar to the estimates provided by Channell et al. (2003) and Hüsing et al. (2011). Option #2 implies average values of sediment accumulation rates at Pizzo Mondello of ~30 m/m.y. for the Carnian–Norian boundary interval from the section base up to 146.5 m, and of ~20 m/m.y. for Norian (Lacian–Sevatian) strata from 158 m to the section top (Fig. 8A; see Fig. 5 for location of stratigraphic intervals). These figures allow us to directly migrate the $\delta^{13}C$ and $\delta^{18}O$ records from Pizzo Mondello to the (Newark) time domain by simple linear fit of Newark–Pizzo Mondello magnetostratigraphic tie points (Fig. 8A; age-depth tie points in Supplementary Table 2).

Please cite this article as: Muttoni, G., et al., A Middle–Late Triassic (Ladinian–Rhaetian) carbon and oxygen isotope record from the Tethyan Ocean, Palaeogeogr. Palaeoclimatol. Palaeoecol. (2014), http://dx.doi.org/10.1016/j.palaeo.2014.01.018

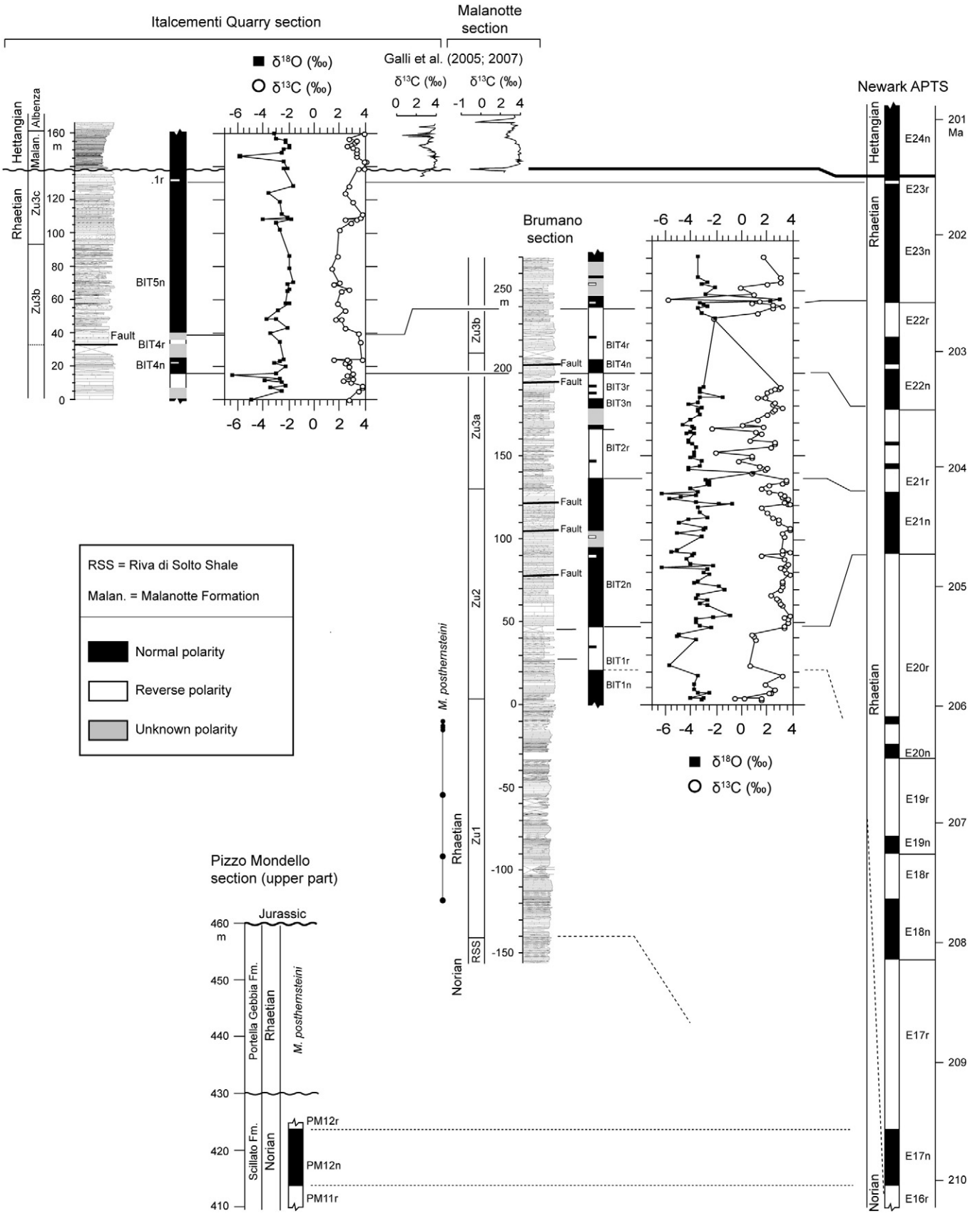

Fig. 7. Brumano and Italcementi Quarry sections: age, lithology, magnetostratigraphy, conodont biostratigraphy, bulk-rock $\delta^{13}C$ and $\delta^{18}O$ data, and correlation to the Newark Astrochronological Polarity Time Scale (APTS). The Newark APTS is here anchored to a Triassic–Jurassic (Rhaetian–Hettangian) boundary at ~201.5 Ma (Blackburn et al., 2013). The Norian–Rhaetian boundary (FAD of *Misikella posthernsteini*) is tentatively placed on the Newark APTS at ~207–210 Ma (nominal age of ~209 Ma) according to correlation of the upper part of the Pizzo Mondello section to the Newark APTS (Muttoni et al., 2010) and correlation of the Steinbergkogel section to the Newark APTS (Hüsing et al., 2011).

Please cite this article as: Muttoni, G., et al., A Middle–Late Triassic (Ladinian–Rhaetian) carbon and oxygen isotope record from the Tethyan Ocean, Palaeogeogr. Palaeoclimatol. Palaeoecol. (2014), http://dx.doi.org/10.1016/j.palaeo.2014.01.018

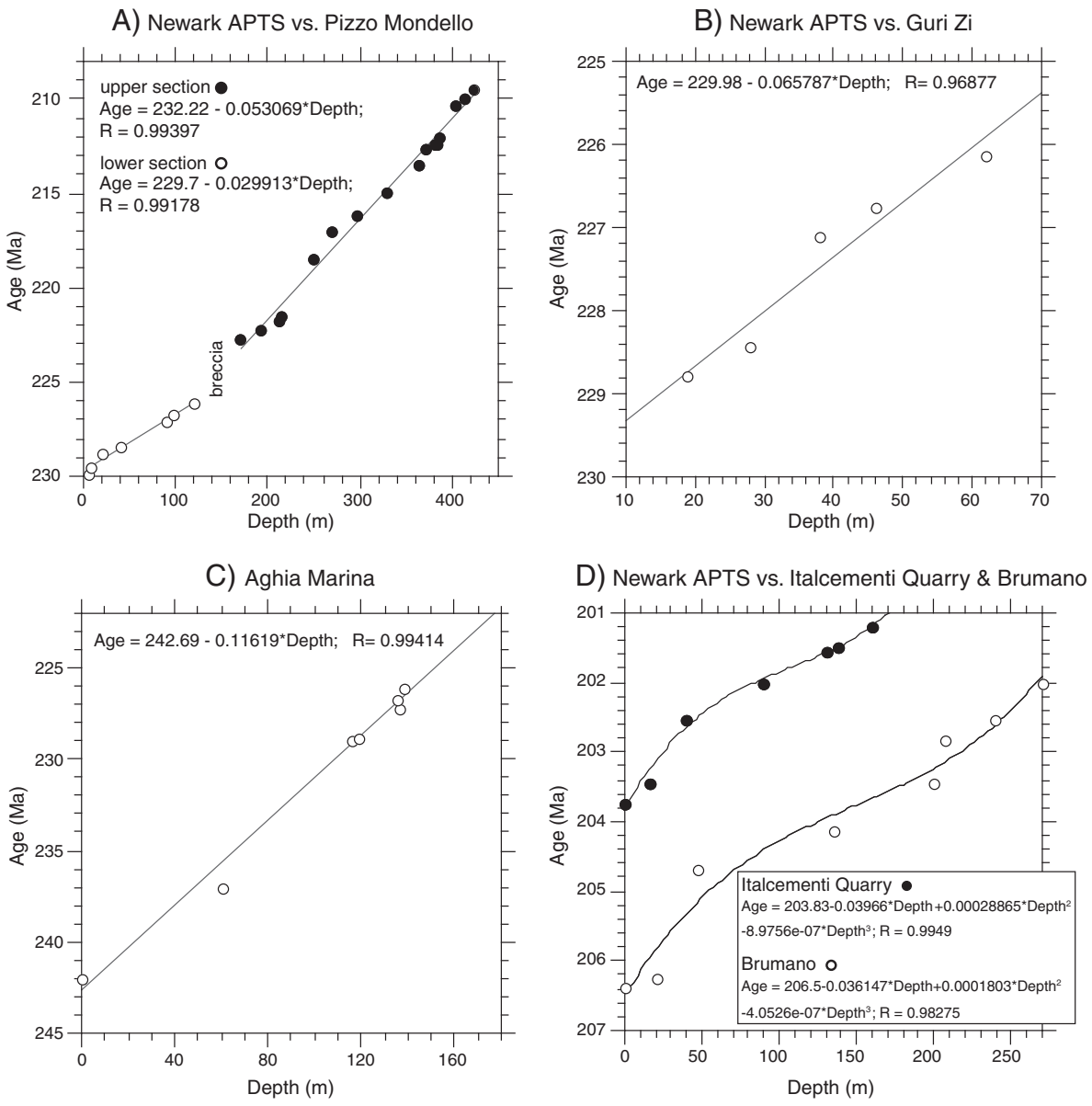

Fig. 8. Age models of sedimentation for Pizzo Mondello (A), Guri Zi (B), Aghia Marina (C), and Brumano and Italcementi Quarry (D). See text for discussion.

The Guri Zi section was also magnetostratigraphically correlated to the Newark APTS in the E6–E8 magnetozone interval (Supplementary Fig. 1B). Using this correlation, we generated an age model for the stable isotope record of Guri Zi by applying a linear best fit to the Newark–Guri Zi magnetostratigraphic tie points (Fig. 8B; age-depth tie points in Supplementary Table 2).

In order to estimate the time window covered by the Aghia Marina section, we applied a linear best fit to the following age-depth tie points (Fig. 8C): (1) an estimated age of ~242 Ma for the Anisian–Ladinian boundary at the base of the section (0 m) based on U/Pb zircon age data from Monte San Giorgio and additional sections from the Dolomites, Italy (Mundil et al., 2010); (2) an estimated age of ~237 Ma for the Ladinian–Carnian boundary at ~60 m based on U/Pb zircon age data from the Carnian global stratotype area of Stuores, Dolomites (Mietto et al., 2012); (3) the ages of the following conodont events derived from magnetostratigraphic correlation of the Pizzo Mondello conodont distribution with the Newark APTS (Supplementary Table 3): ~228.95 Ma for the LAD of *Carnepigondolella nodosa* and ~228.9 Ma for the LAD of *Paragondolella polygnathiformis*, ~227.25 Ma for the FAD *Epigondolella quadrata*, primitive form, which approximates the Carnian–Norian boundary, ~226.8 Ma for the FAD of *Carnepigondolella gulloae*, and ~226.2 Ma for the LAD of *C. gulloae.*

Finally, the age models of sedimentation of the Brumano and Italcementi Quarry sections are based on third-order polynomial

Fig. 9. The Middle–Late Triassic (Ladinian–Rhaetian) $\delta^{13}C$ records from Aghia Marina, Guri Zi, Pizzo Mondello, Brumano, and Italcementi Quarry (A), illustrated in detail across the Carnian–Norian boundary (B) and in the Rhaetian (C), have been compared to $\delta^{13}C$ data from Korte et al. (2005) (D) on whole rock, brachiopods (Mn < 250 ppm and/or Sr > 400 ppw), and aragonitic fossils from various Tethyan marine sections. The Korte et al. (2005) record is scaled to the time scale of panel (A) using a Carnian–Norian boundary at 227 Ma, a Norian–Rhaetian boundary at 229.5 Ma, and a Triassic–Jurassic (Rhaetian–Hettangian) boundary at 201.5 Ma. See text for discussion.

Please cite this article as: Muttoni, G., et al., A Middle–Late Triassic (Ladinian–Rhaetian) carbon and oxygen isotope record from the Tethyan Ocean, Palaeogeogr. Palaeoclimatol. Palaeoecol. (2014), http://dx.doi.org/10.1016/j.palaeo.2014.01.018

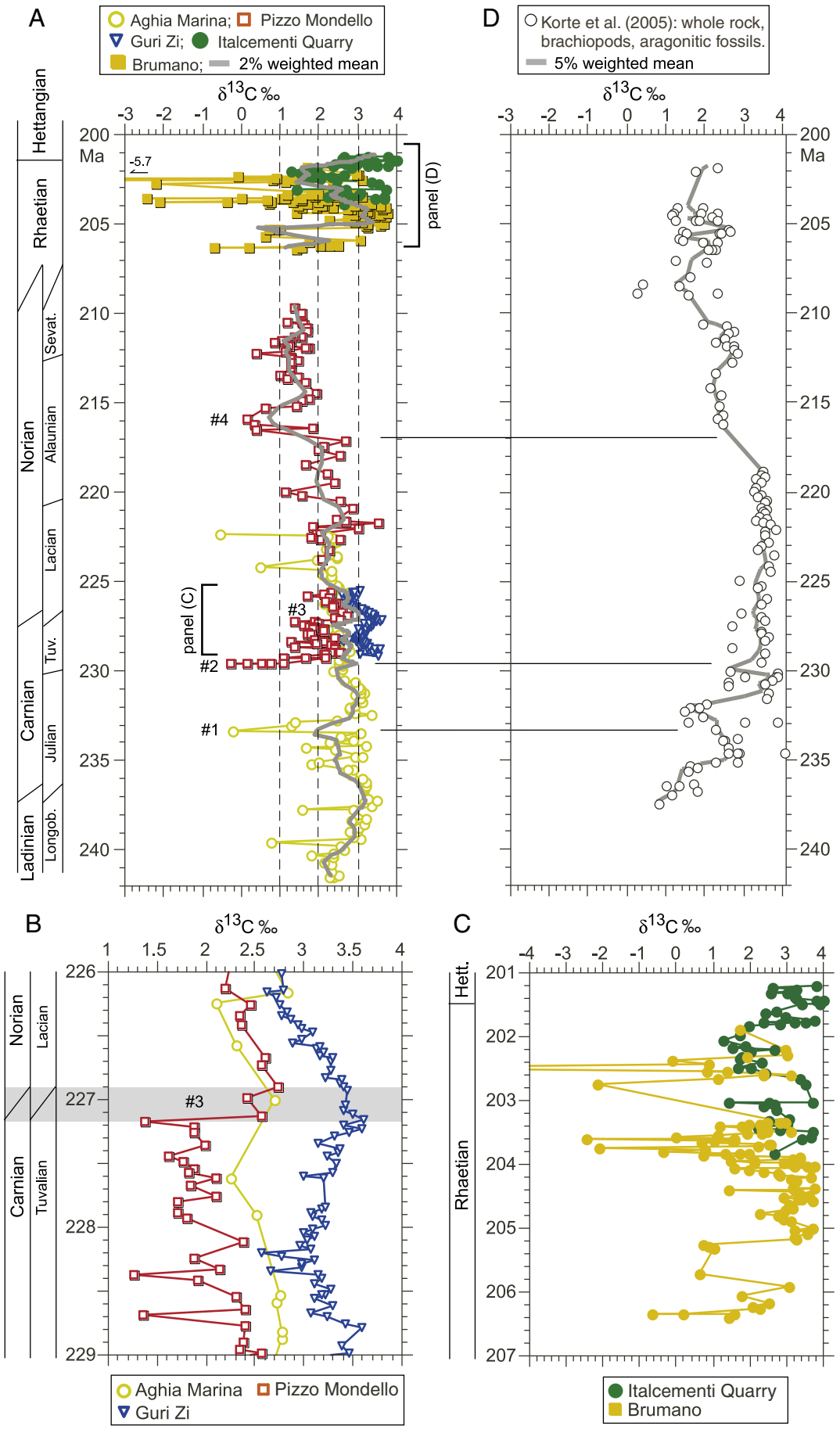

Please cite this article as: Muttoni, G., et al., A Middle–Late Triassic (Ladinian–Rhaetian) carbon and oxygen isotope record from the Tethyan Ocean, Palaeogeogr. Palaeoclimatol. Palaeoecol. (2014), http://dx.doi.org/10.1016/j.palaeo.2014.01.018

functions fitted to the age-depth tie points derived from magnetostratigraphic correlation with the Newark APTS (Muttoni et al., 2010) (Fig. 8D; age-depth tie points in Supplementary Table 2).

7. A composite Ladinian–Rhaetian $\delta^{13}C_{carb}$ record

Using the age models illustrated above, we generated $\delta^{13}C$ and $\delta^{18}O$ records encompassing more than 40 Myr of the Middle–Late Triassic (Ladinian–Rhaetian). The $\delta^{18}O$ records from Aghia Marina, Pizzo Mondello, Guri Zi, and Brumano–Italcementi Quarry (Supplementary Fig. 2) show non-reproducible values across overlapping sections of broadly similar lithology, thus suggesting that diagenesis (e.g., recrystallization) may have altered the original equilibrium values.

The carbon signal, generally considered more resistant to diagenetic alteration than oxygen, is interpreted as largely representative of the original carbon isotope composition of the near-surface waters of the Tethys Ocean. This is because the analyzed sediments are either pelagic limestones containing calcareous nannofossils (Preto et al., 2012) or resedimented carbonate platform micrites, or shallow-water limestones (but see discussion on possible mixing of carbon from different sources in the Rhaetian Brumano section). We note that relatively little sedimentary carbonate is produced in deep waters, and therefore bulk sediment/rock samples best characterize the average $\delta^{13}C$ of the total carbonate produced and preserved in the marine system (Shackleton, 1987). Despite differences in absolute isotopic values between Aghia Marina, Pizzo Mondello, and Guri Zi (e.g., across the Carnian–Norian boundary; see below), or the apparently erratic Rhaetian record at Brumano, which may reflect local contributions to a global carbon signal, we believe that some of the excursions observed in our composite record, as well as the long-term trend that characterizes it, may be primary chemostratigraphic features as revealed from correlations with other studies from the literature.

Aghia Marina data show $\delta^{13}C$ values increasing by ~1‰ in the Ladinian (Longobardian) followed by an ~0.6‰ decrease across the Ladinian–Carnian boundary. This is followed by relatively constant (albeit oscillatory) values during the Carnian, punctuated by three main excursions: at ~233 Ma in the early Carnian (Julian) in the Aghia Marina record (#1; Fig. 9A), at ~229.5 Ma across the early–late Carnian (Julian–Tuvalian) boundary in the Pizzo Mondello record (#2; Fig. 9A), and at ~227 Ma across the Carnian–Norian boundary at Pizzo Mondello and Guri Zi (#3; Fig. 9A; enlarged in Fig. 9B). Above this, a long-term decreasing trend of ~1.5‰ in the Norian (Aghia Marina, Pizzo Mondello) is punctuated by additional oscillations and a fourth main excursion at ~216 Ma in the middle Norian (Alaunian) (#4; Fig. 9A). Finally, after a late Norian–early Rhaetian gap, $\delta^{13}C$ values increase in the Rhaetian compared to average Norian values, and are characterized by large single-sample increases and decreases (Fig. 9A; enlarged in Fig. 9C).

We compare our $\delta^{13}C$ composite record with records from the literature that use various combinations of brachiopod and bulk rock analyses from Triassic sections (e.g., Hayes et al., 1999; Veizer et al., 1999; Payne et al., 2004; Korte et al., 2005; Preto et al., 2012).

The Ladinian increase at Aghia Marina is broadly consistent (within a temporal resolution of ~2–3 Myr) with a late Anisian–Carnian trend identified in South China bulk rock samples (Payne et al., 2004) and Tethyan Alps bulk rock and brachiopod $\delta^{13}C$ records (Preto et al., 2005). The Ladinian–Carnian boundary decrease at Aghia Marina is also consistent with an ~1‰ decrease in the earliest Carnian at two locations (Preto et al., 2012). The wide scatter at this level makes it difficult to discern whether this decrease is also recorded in the Korte et al. (2005) record (Fig. 9D).

The negative excursion at ~233 Ma in the early Carnian (Julian) (#1; Fig. 9A) seems to correlate with the Carnian negative excursion present in the Korte et al. (2005) data (Fig. 9D), and is broadly compatible in age with the negative $\delta^{13}C$ spike recently observed in sections from the Dolomites and tentatively correlated with the eruption of the Wrangellia flood basalts (Dal Corso et al., 2012). The negative excursion found at Pizzo Mondello at ~229.5 Ma (#2; Fig. 9A) seems to correspond to a late Carnian negative excursion present in the Korte et al. (2005) data (Fig. 9D); this excursion is not present in correlative levels at Aghia Marina, where sampling resolution is lower compared to Pizzo Mondello. This negative $\delta^{13}C$ excursion may have resulted from rapid transfer of ^{12}C-enriched carbon to the mobile carbon reservoirs or decreases in organic carbon burial or climate-modulated productivity increases.

The Carnian–Norian boundary positive excursion (Fig. 9B) is registered at both Pizzo Mondello and Guri Zi (albeit with different details), whereas at Aghia Marina (as well as in the Korte et al. (2005) record; Fig. 9D), it appears subdued possibly due to lower sampling resolution. This positive $\delta^{13}C$ excursion may have arisen from increases in organic carbon burial or climate-modulated productivity decreases.

The Norian decline in $\delta^{13}C$ values recorded at Pizzo Mondello (Fig. 9A) is reminiscent of the Korte et al. (2005) record, in which late Norian $\delta^{13}C$ values are ~1‰ lower than in the early Norian (Fig. 9D). $\delta^{13}C$ values from Pizzo Mondello are on average ~1.5‰ lower than whole-rock data from the Silicka Brezova section used in Korte et al. (2005), suggesting that different depositional histories between the

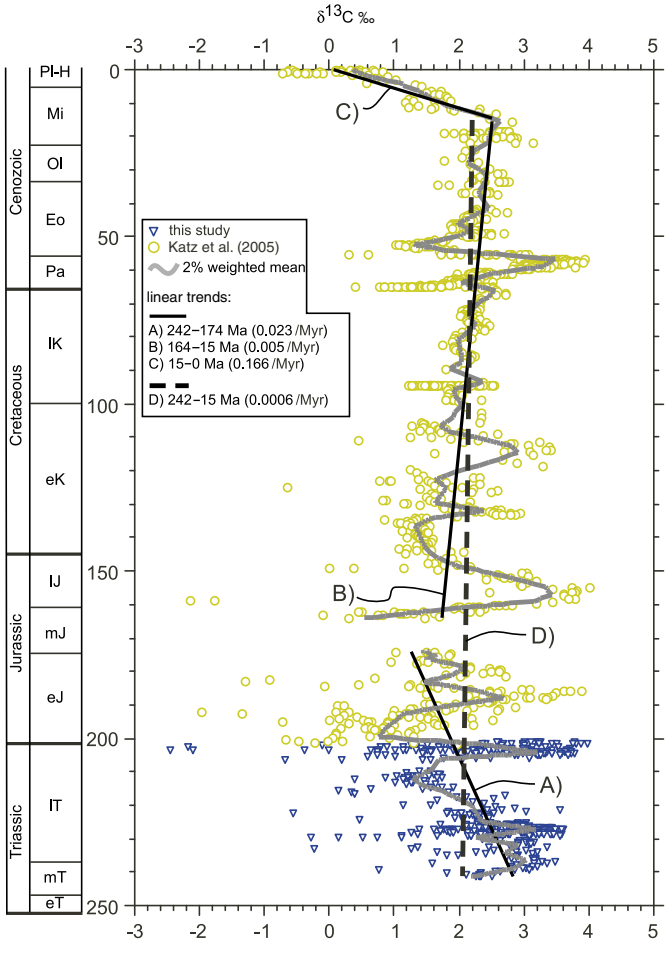

Fig. 10. The Middle–Late Triassic (Ladinian–Rhaetian) $\delta^{13}C$ record of this study has been appended to the Jurassic–Recent bulk sediment data compiled by Katz et al. (2005) in order to provide a composite $\delta^{13}C$ record spanning the last ~242 Myr of Earth's history and showing oscillations and trends useful for stratigraphic correlations and for a better understanding of the global carbon cycle. The Katz et al. (2005) record is calibrated to the time scales of Berggren et al. (1995) for the Cenozoic, and Gradstein et al. (1995) for the Cretaceous–Middle Jurassic, whereas for the Early Jurassic (Hettangian–Toarcian), it has been here re-scaled adopting an Early–Middle Jurassic (Toarcian–Aalenian) boundary at 174.1 Ma and a Triassic–Jurassic (Rhaetian–Hettangian) boundary at 201.5 Ma. Acronyms: eT = early Triassic, mT = middle Triassic, lT = late Triassic, eJ = early Jurassic, mJ = middle Jurassic, lJ = late Jurassic, eK = early Cretaceous, lK = late Cretaceous, Pa = Paleocene, Eo = Eocene, Ol = Oligocene, Mi = Miocene, Pl–H = Pliocene–Holocene. See text for discussion.

two sections may have variably impacted the overall $\delta^{13}C$ values; nonetheless, a global signal seems to be preserved. This overall trend is punctuated by a negative excursion observed in the Pizzo Mondello record at ~216 Ma in the middle Norian (Alaunian) (#4; Fig. 9A).

The Rhaetian is characterized by $\delta^{13}C$ values that are on average higher compared to the Norian (Fig. 9A). Rhaetian values initially increase to ~3.4‰, followed by a decrease of ~2‰ and a subsequent return to ~3.4‰ (Fig. 9A). Within these trends, which seem to be supported by the Rhaetian (low resolution) record of Palfy et al. (2001) from Hungary, several single-sample increases and decreases of up to ~5–6‰ are embedded (Fig. 9C). It is unclear whether this 'erratic' behavior of the Rhaetian $\delta^{13}C$ record reflects a true signal of the global carbon cycle, or whether it is in part due to local mixing of different sources of carbonate carbon with different $\delta^{13}C$ values in the Brumano section, which is characterized by variable lithologies arranged in shallow- to deeper-water cyclic patterns of sedimentation of different orders and scales (Muttoni et al., 2010). However, we note that Palfy et al. (2001) recorded ~5–6‰ changes in a lower-resolution Rhaetian record.

8. Towards a composite Triassic–Present $\delta^{13}C_{carb}$ record

Our Triassic $\delta^{13}C$ record has been appended to the Jurassic–Recent bulk sediment $\delta^{13}C$ record compiled by Katz et al. (2005) that mainly reflects calcareous plankton and the total carbonate transferred from the oceans to marine sediments through time. The resulting composite record (Fig. 10), spanning the last ~242 Myr of Earth's history, shows multimillion year $\delta^{13}C$ fluctuations around longer-term trends. From ~242 Ma in the Middle Triassic to ~174 Ma at the end of the Early Jurassic, $\delta^{13}C$ values decrease on the long term by ~1.5‰ (Fig. 10, linear trend A), indicating some combination of decreases in productivity and burial of organic matter, or transfer of ^{12}C-enriched organic matter from continental margins or terrestrial environments to mobile carbon reservoirs during the low sea level associated with the supercontinent Pangea. From ~164 Ma in the Middle Jurassic to ~15 Ma in the Miocene, there is a long-term increase of ~1‰ (Fig. 10, linear trend B), previously described by Katz et al. (2005), which they attribute to a combination of increases in productivity and burial of organic matter associated with the break-up of Pangea and expansion of large-celled eukaryotic phytoplankton, which are significant contributors to export productivity. Finally, since ~15 Ma, $\delta^{13}C$ data plummet to modern values of ~0‰ or less (Fig. 10, linear trend C), depicting a sustained decrease of the global carbon cycle (Broecker and Woodruff, 1992) that was interpreted by Katz et al. (2005) as in part due to the rise of C4 photosynthetic pathways and in part to erosion and weathering of organic-rich shales.

The long-term compilation presented in this study reveals an interesting component of the carbon cycle not previously noted (Fig. 10). A least-square best-fit line drawn through the whole 242–15 Ma (or even 242–0 Ma) dataset shows that there is no long-term trend, with $\delta^{13}C$ values varying around a mean of ~2‰ (Fig. 10, linear trend D). This suggests that over very long time scales (10^8 yr or higher), the carbon cycle is at dynamic (i.e., oscillatory) steady state, as observed also in the Paleozoic (Veizer et al., 1999) or even Pre-Cambrian (Prokoph et al., 2008) record. An important implication of this is that carbon production and recycling through biological and geological processes average out through supercontinent cycles.

9. Conclusions

1) New conodont biostratigraphic data are presented from the well-exposed Aghia Marina marine limestone section from Greece that encompasses in continuity a substantial portion of the Triassic from the Ladinian to the Norian.
2) The conodont biostratigraphy from the coeval Pizzo Mondello marine section from Sicily and the Guri Zi section from Albania has been revised and updated after recent improvements in the taxonomy of Late Triassic conodonts.
3) On these Ladinian–Norian sections, as well as on two additional Rhaetian sections from the Southern Alps of Italy (Brumano and Italcementi Quarry), we obtained bulk-sediment $\delta^{18}O$ and $\delta^{13}C$ data that we migrated from the depth to the time domain using available chronostratigraphic tie points, obtaining Ladinian–Rhaetian $\delta^{13}C$ and $\delta^{18}O$ composite records spanning from ~242 Ma to ~201 Ma.
4) Whereas the $\delta^{18}O$ record seems to be affected by diagenesis, the $\delta^{13}C$ record appears to preserve a primary signal and shows values increasing by ~1‰ in the Ladinian followed by an ~0.6‰ decrease across the Ladinian–Carnian boundary, followed by relatively constant (but oscillatory) Carnian values punctuated by three main excursions: a negative excursion at ~233 Ma in the early Carnian, a second negative excursion at ~229.5 Ma across the early–late Carnian boundary, and a positive excursion at ~227 Ma across the Carnian–Norian boundary. The Norian is characterized by a decreasing trend punctuated by a negative excursion at ~216 Ma in the middle Norian. Rapid increases and decreases in $\delta^{13}C$ have been observed in the Rhaetian from ~207 Ma to ~201 Ma, but these are provisionally considered at least in part due to mixing of different sources of carbonate carbon with different $\delta^{13}C$ values.
5) Our Middle–Late Triassic $\delta^{13}C$ record, appended to the Jurassic–Recent bulk sediment $\delta^{13}C$ record of Katz et al. (2005), provides a largely continuous record from ~242 Ma to the Present that reveals multimillion year oscillations around longer-term trends: from ~242 Ma to ~174 Ma, $\delta^{13}C$ values seem to decrease by ~1.5‰, whereas from ~164 Ma up to ~15 Ma, $\delta^{13}C$ values seem to increase by ~1‰, as previously described by Katz et al. (2005). A final rapid decrease to modern $\delta^{13}C$ values of around 0‰ occurs since ~15 Ma, and was interpreted by Katz et al. (2005) as due to the rise of C4 photosynthetic pathways and/or to unburial and weathering of organic-rich shales. If the whole dataset from 242 to 15 Ma (or even 0 Ma) is considered, these opposing long-term trends balance each other out, and no increase or decrease of $\delta^{13}C$ is observed, suggesting that at this very long time scale, the carbon cycle may be at a dynamic steady state.

Supplementary data to this article can be found online at http://dx.doi.org/10.1016/j.palaeo.2014.01.018.

Acknowledgments

Two anonymous reviewers are thanked for insightful comments that improved the manuscript. Acknowledgment is made to the donors of the American Chemical Society Petroleum Research Fund for partial support of this research to M.E.K. (grant 49637-DN18), and to PRIN 2008 '*Stratigrafia integrata del Triassico Superiore: GSSP e sezioni ausiliarie in Italia*' for partial support to M.B.

References

Angiolini, L., Dragonetti, L., Muttoni, G., Nicora, A., 1992. Triassic stratigraphy of the Island of Hydra (Greece). Riv. Ital. Paleontol. Stratigr. 98 (2), 137–180.
Balini, M., 1994. Middle Triassic ceratitids (Ammonoidea) collected by C. Renz from Hydra (Greece). Riv. Ital. Paleontol. Stratigr. 100, 351–364.
Balini, M., Bertinelli, A., Di Stefano, P., Guaiumi, C., Levera, M., Mazza, M., Muttoni, G., Nicora, A., Preto, N., Rigo, M., 2010. The Late Carnian–Rhaetian succession at Pizzo Mondello (Sicani Mountains). Albertiana 39, 36–58.
Balini, M., Krystyn, L., Levera, M., Tripodo, A., 2012. Late Carnian–Early Norian ammonoids from the GSSP candidate section Pizzo Mondello (Sicani Moutains, Sicily). Riv. Ital. Paleontol. Stratigr. 118, 47–84.
Baumgartner, P.O., 1985. Jurassic Sedimetary Evolution and Nappe Emplacement in the Argolis Peninsula (Peloponnesus, Greece). Springer.
Berggren, W.A., Kent, D.V., Swisher, C.C., Aubry, M.-P., 1995. A revised Cenozoic geochronology and chronostratigraphy. In: Berggren, W.A., Kent, D.V., Hardenbol, J. (Eds.), Geochronology, Time Scales and Global Stratigraphic Correlations: A Unified Temporal Framework for a Historical Geology. SEPM (Society for Sedimentary Geology), Tulsa, OK, pp. 129–212.
Blackburn, T.J., Olsen, P., Bowring, S.A., McLean, N.M., Kent, D.V., Puffer, J., McHone, G., Rasbury, E.T., Et-Touhami, M., 2013. Zircon U–Pb geochronology links the end-Triassic extinction with the Central Atlantic Magmatic Province. Science 340, 941–945.

Broecker, W.S., Woodruff, F., 1992. Discrepancies in the oceanic carbon isotope record for the last fifteen million years? Geochim. Cosmochim. Acta 56, 3259–3264.

Channell, J.E.T., Kozur, H.W., Sievers, T., Mock, R., Aubrecht, R., 2003. Carnian–Norian biomagnetostratigraphy at Silicka Brezova (Slovakia): correlation to other Tethyan sections and to the Newark Basin. Palaeogeogr. Palaeoclimatol. Palaeoecol. 191, 65–109.

Coplen, T.B., 1995. Discontinuance of SMOW and PDB. Nature 375, 285.

Dal Corso, J., Mietto, P., Newton, R.J., Pancost, R.D., Preto, N., Roghi, G., Wignall, P.B., 2012. Discovery of a major negative $\delta^{13}C$ spike in the Carnian (Late Triassic) linked to the eruption of Wrangellia flood basalts. Geology 40, 79–82.

Epstein, A.G., Epstein, J.B., Harris, L.D., 1977. Conodont color alteration: an index to organic metamorphism. U. S. Geol. Surv. Prof. Pap. 995, 27.

Gallet, Y., Krystyn, L., Marcoux, J., Besse, J., 2007. New constraints on the end-Triassic (Upper Norian–Rhaetian) magnetostratigraphy. Earth Planet. Sci. Lett. 255, 458–470.

Galli, M.T., Jadoul, F., Bernasconi, S.M., Weissert, H., 2005. Anomalies in global carbon cycling at the Triassic/Jurassic boundary: evidence from a marine C-isotope record. Palaeogeogr. Palaeoclimatol. Palaeoecol. 216, 203–214.

Galli, M.T., Jadoul, F., Bernasconi, S.M., Cirilli, S., Weissert, H., 2007. Stratigraphy and palaeoenvironmental analysis of the Triassic–Jurassic transition in the western Southern Alps (Northern Italy). Palaeogeogr. Palaeoclimatol. Palaeoecol. 244, 52–70.

Gradstein, F.M., Agterberg, F.P., Ogg, J.G., Hardenbol, H., van Veen, P., Thierry, J., Huang, Z., 1995. A Triassic, Jurassic, and Cretaceous time scale. In: Berggren, W.A., Kent, D.V., Hardenbol, J. (Eds.), Geochronology, Time Scales and Global Stratigraphic Correlations: A Unified Temporal Framework for a Historical Geology. SEPM (Society for Sedimentary Geology), Tulsa, OK, pp. 95–126.

Hayashi, S., 1968. The Permian conodonts in chert of the Adoyama Formation, Ashio Mountains, central Japan. Earth Sci. 22 (2), 63–77.

Hayes, J.M., Strauss, H., Kaufman, A.J., 1999. The abundance of 13C in marine organic matter and isotopic fractionation in the global biogeochemical cycle of carbon during the past 800 Ma. Chem. Geol. 161, 103–125.

Hounslow, M.W., Muttoni, G., 2010. The geomagnetic polarity timescale for the Triassic: linkage to stage boundary definitions. Geol. Soc. Lond. Spec. Publ. 334, 61–102.

Hüsing, S.K., Deenen, M.H., Koopmans, J.G., Krijgsman, W., 2011. Magnetostratigraphic dating of the proposed Rhaetian GSSP at Steinbergkogel (Upper Triassic, Austria): implications for the Late Triassic time scale. Earth Planet. Sci. Lett. 302, 203–216.

Katz, M.E., Wright, J.D., Miller, K.G., Cramer, B.S., Fennel, K., Falkowski, P.G., 2005. Biological overprint of the geological carbon cycle. Mar. Geol. 217, 323–338.

Kent, D.V., Olsen, P.E., 1999. Astronomically tuned geomagnetic polarity time scale for the Late Triassic. J. Geophys. Res. 104, 12,831–812,841.

Korte, C., Kozur, H.W., Veizer, J., 2005. $\delta^{13}C$ and $\delta^{18}O$ values of Triassic brachiopods and carbonate rocks as proxies for coeval seawater and palaeotemperature. Palaeogeogr. Palaeoclimatol. Palaeoecol. 226, 287–306.

Kozur, H., 2003. Integrated ammonoid-, conodont and radiolarian zonation of the Triassic. Hallesches Jahrb. Geowiss. 25, 49–79.

Krystyn, L., Gallet, Y., Besse, J., Marcoux, J., 2002. Integrated Upper Carnian to Lower Norian biochronology and implications for the Upper Triassic magnetic polarity time scale. Earth Planet. Sci. Lett. 203, 343–351.

Marshall, J.D., 1992. Climatic and oceanographic isotopic signals from the carbonate rock record and their preservation. Geol. Mag. 129 (2), 143–160.

Martini, R., Zaninetti, L., Abate, B., Renda, P., Doubinger, J., Rauscher, R., Vrielynck, B., 1991. Sédimentologie et biostratigraphie de la formation triasique Mufara (Sicile occidentale): foraminiféres, conodontes, palynomorphes. Riv. Ital. Paleontol. Stratigr. 97 (2), 131–152.

Mazza, M., Furin, S., Spötl, C., Rigo, M., 2010. Generic turnovers of Carnian/Norian conodonts: climatic control or competition? Palaeogeogr. Palaeoclimatol. Palaeoecol. 290, 120–137.

Mazza, M., Rigo, M., Nicora, A., 2011. A new Metapolygnathus platform conodont species and its implications for Upper Carnian global correlations. Acta Palaeontol. Pol. 56 (1), 121–131.

Mazza, M., Rigo, M., Gullo, M., 2012a. Taxonomy and biostratigraphic record of the Upper Triassic conodonts of the Pizzo Mondello section (western Sicily, Italy), GSSP candidate for the base of the Norian. Riv. Ital. Paleontol. Stratigr. 118 (1), 85–130.

Mazza, M., Cau, A., Rigo, M., 2012b. Application of numerical cladistic analyses to the Carnian–Norian conodonts: a new approach for phylogenetic interpretations. J. Syst. Palaeontol. 10, 401–422.

Mietto, P., Manfrin, S., Preto, N., Rigo, M., Roghi, G., Furin, S., Gianolla, P., Posenato, R., Muttoni, G., Nicora, A., Buratti, N., Cirilli, S., Spötl, C., Ramezani, J., Bowring, S.A., 2012. The Global Boundary Stratotype Section and Point (GSSP) of the Carnian Stage (Late Triassic) at Prati di Stuores/Stuores Wiesen Section (Southern Alps, NE Italy). Episodes 35, 414–430.

Moix, P., Kozur, H.W., Stampfli, G.M., Mostler, H., 2007. New paleontological, biostratigraphic and paleogeographic results from the Triassic of the Mersin Mélange, SE Turkey. N. M. Mus. Nat. Hist. Sci. Bull. 41, 282–311.

Mundil, R., Palfy, J., Renne, P.R., Brack, P., 2010. The Triassic timescale: new constraints and a review of geochronological data. Geol. Soc. Lond. Spec. Publ. 334, 41–60.

Muttoni, G., Channell, J.E.T., Nicora, A., Rettori, R., 1994. Magnetostratigraphy and biostratigraphy of an Anisian–Ladinian (Middle Triassic) boundary section from Hydra (Greece). Palaeogeogr. Palaeoclimatol. Palaeoecol. 111, 249–262.

Muttoni, G., Kent, D.V., Brack, P., Nicora, A., Balini, M., 1997. Middle Triassic magnetostratigraphy and biostratigraphy from the Dolomites and Greece. Earth Planet. Sci. Lett. 146, 107–120.

Muttoni, G., Kent, D.V., Di Stefano, P., Gullo, M., Nicora, A., Tait, J., Lowrie, W., 2001. Magnetostratigraphy and biostratigraphy of the Carnian/Norian boundary interval from the Pizzo Mondello section (Sicani Mountains, Sicily). Palaeogeogr. Palaeoclimatol. Palaeoecol. 166, 383–399.

Muttoni, G., Kent, D.V., Olsen, P.E., Di Stefano, P., Lowrie, W., Bernasconi, S., Martín Hernández, F., 2004. Tethyan magnetostratigraphy from Pizzo Mondello (Sicily) and correlation to the Late Triassic Newark astrochronological polarity time scale. Geol. Soc. Am. Bull. 116, 1043–1058.

Muttoni, G., Meco, S., Gaetani, M., 2005. Carnian–Norian boundary magneto-biostratigraphy from Guri Zi (Albania). Riv. Ital. Paleontol. Stratigr. 111, 233–245.

Muttoni, G., Kent, D.V., Jadoul, F., Olsen, P.E., Rigo, M., Galli, M.T., Nicora, A., 2010. Rhaetian magneto-biostratigraphy from the Southern Alps (Italy): constraints on Triassic chronology. Palaeogeogr. Palaeoclimatol. Palaeoecol. 285, 1–16.

Nicora, A., Balini, M., Bellanca, A., Bertinelli, A., Bowring, S.A., Di Stefano, P., Dumitrica, P., Guaiumi, C., Gullo, M., Hungerbuehler, A., Levera, M., Mazza, M., McRoberts, C.A., Muttoni, G., Preto, N., Rigo, M., 2007. The Carnian/Norian boundary interval at Pizzo Mondello (Sicani Mountains, Sicily) and its bearing for the definition of the GSSP of the Norian Stage. Albertiana 36, 102–115.

Noyan, O., Kozur, H., 2007. Revision of the late Carnian–early Norian conodonts from the Stefanion section (Argolis, Greece) and their paleobiogeographic implications. N. Jb. Geol. Paläont. (Abh.) 245 (2), 159–178.

Olsen, P.E., Kent, D.V., 1999. Long-period Milankovitch cycles from the Late Triassic and Early Jurassic of eastern North America and their implications for the calibration of the Early Mesozoic time-scale and the long-term behaviour of the planets. Philos. Trans. R. Soc. Lond. Ser. A 357, 1761–1786.

Palfy, J., Demeny, A., Haas, J., Hetenyi, M., Orchard, M.J., Veto, I., 2001. Carbon isotope anomaly and other geochemical changes at the Triassic–Jurassic boundary from a marine section in Hungary. Geology 29, 1047–1050.

Payne, J.L., Lehrmann, D.J., Wei, J., Orchard, M.J., Schrag, D.P., Knoll, A.H., 2004. Large perturbations of the carbon cycle during recovery from the end-Permian extinction. Nature 305, 506–509.

Preto, N., Spötl, C., Gianolla, P., Mietto, P., Riva, A., Manfrin, S., 2005. Aragonite dissolution, sedimentation rates and carbon isotopes in deep-water hemipelagites (Livinallongo Formation, Middle Triassic, northern Italy). Sediment. Geol. 181, 173–194.

Preto, N., Rigo, M., Agnini, C., Bertinelli, A., Guaiumi, C., Borello, S., Westphal, H., 2012. Triassic and Jurassic calcareous nannofossils of the Pizzo Mondello section: a SEM study. Riv. Ital. Paleontol. Stratigr. 118 (1), 131–141.

Prokoph, A., Shields, G., Veizer, J., 2008. Compilation and time-series analysis of a marine carbonate delta O-18, delta C-13, Sr-87/Sr-86 and delta S-34 database through Earth history. Earth-Sci. Rev. 87, 113–133.

Renz, C., 1931. Die Bulogkalke der Insel Hydra (Ostpeloponnes). Eclogae Geol. Helv. 24, 53–60.

Shackleton, N.J., 1987. Oxygen isotopes, ice volume and sea level. Quat. Sci. Rev. 6, 183–190.

Swart, P.K., 2008. Global synchronous changes in the carbon isotopic composition of carbonate sediments unrelated to changes in the global carbon cycle. Proc. Natl. Acad. Sci. 105 (37), 13741–13745.

Veizer, J., Ala, K., Azmy, K., Bruckschen, P., Buhl, D., Bruhn, F., Carden, G.A.F., Diener, A., Ebneth, S., Godderis, Y., Jasper, T., Korte, C., Pawellek, F., Podlaha, O.G., Strauss, H., 1999. $^{87}Sr/^{86}Sr$, $\delta^{13}C$ and $\delta^{18}O$ evolution of Phanerozoic seawater. Chem. Geol. 161, 59–88.

Please cite this article as: Muttoni, G., et al., A Middle–Late Triassic (Ladinian–Rhaetian) carbon and oxygen isotope record from the Tethyan Ocean, Palaeogeogr. Palaeoclimatol. Palaeoecol. (2014), http://dx.doi.org/10.1016/j.palaeo.2014.01.018